

# PWM Switching Frequency Effects on Eddy Current Sensors for Magnetically Suspended Flywheel Systems

Ralph Jansen University of Toledo, Toledo, Ohio

Ramon Lebron Glenn Research Center, Cleveland, Ohio

Tim Dever QSS Group, Inc., Cleveland, Ohio

Art Birchenough Glenn Research Center, Cleveland, Ohio Since its founding, NASA has been dedicated to the advancement of aeronautics and space science. The NASA Scientific and Technical Information (STI) Program Office plays a key part in helping NASA maintain this important role.

The NASA STI Program Office is operated by Langley Research Center, the Lead Center for NASA's scientific and technical information. The NASA STI Program Office provides access to the NASA STI Database, the largest collection of aeronautical and space science STI in the world. The Program Office is also NASA's institutional mechanism for disseminating the results of its research and development activities. These results are published by NASA in the NASA STI Report Series, which includes the following report types:

- TECHNICAL PUBLICATION. Reports of completed research or a major significant phase of research that present the results of NASA programs and include extensive data or theoretical analysis. Includes compilations of significant scientific and technical data and information deemed to be of continuing reference value. NASA's counterpart of peerreviewed formal professional papers but has less stringent limitations on manuscript length and extent of graphic presentations.
- TECHNICAL MEMORANDUM. Scientific and technical findings that are preliminary or of specialized interest, e.g., quick release reports, working papers, and bibliographies that contain minimal annotation. Does not contain extensive analysis.
- CONTRACTOR REPORT. Scientific and technical findings by NASA-sponsored contractors and grantees.

- CONFERENCE PUBLICATION. Collected papers from scientific and technical conferences, symposia, seminars, or other meetings sponsored or cosponsored by NASA.
- SPECIAL PUBLICATION. Scientific, technical, or historical information from NASA programs, projects, and missions, often concerned with subjects having substantial public interest.
- TECHNICAL TRANSLATION. Englishlanguage translations of foreign scientific and technical material pertinent to NASA's mission.

Specialized services that complement the STI Program Office's diverse offerings include creating custom thesauri, building customized databases, organizing and publishing research results . . . even providing videos.

For more information about the NASA STI Program Office, see the following:

- Access the NASA STI Program Home Page at http://www.sti.nasa.gov
- E-mail your question via the Internet to help@sti.nasa.gov
- Fax your question to the NASA Access Help Desk at 301–621–0134
- Telephone the NASA Access Help Desk at 301–621–0390
- Write to:

NASA Access Help Desk NASA Center for AeroSpace Information 7121 Standard Drive Hanover, MD 21076



# PWM Switching Frequency Effects on Eddy Current Sensors for Magnetically Suspended Flywheel Systems

Ralph Jansen University of Toledo, Toledo, Ohio

Ramon Lebron Glenn Research Center, Cleveland, Ohio

Tim Dever QSS Group, Inc., Cleveland, Ohio

Art Birchenough Glenn Research Center, Cleveland, Ohio

Prepared for the First International Energy Conversion Engineering Conference sponsored by the American Institute of Aeronautics and Astronautics Portsmouth, Virginia, August 17–21, 2003

National Aeronautics and Space Administration

Glenn Research Center

Available from

NASA Center for Aerospace Information 7121 Standard Drive Hanover, MD 21076 National Technical Information Service 5285 Port Royal Road Springfield, VA 22100

## PWM SWITCHING FREQUENCY EFFECTS ON EDDY CURRENT SENSORS FOR MAGNETICALLY SUSPENDED FLYWHEEL SYSTEMS

Ralph H. Jansen University of Toledo Toledo, Ohio Ramon Lebron NASA Glenn Research Center Cleveland, Ohio Timothy P. Dever QSS Group, Inc. Cleveland, Ohio Arthur G. Birchenough NASA Glenn Research Center Cleveland, Ohio

#### Abstract

A flywheel magnetic bearing (MB) pulse width modulated power amplifier (PWM) configuration is selected to minimize noise generated by the PWMs in the flywheel position sensor system. Two types of noise are addressed: beat frequency noise caused by variations in PWM switching frequencies, and demodulation noise caused by demodulation of high order harmonics of the switching voltage into the MB control band. Beat frequency noise is eliminated by synchronizing the PWM switch frequencies, and demodulation noise is minimized by selection of a switching frequency which does not have harmonics at the carrier frequency of the sensor. The recommended MB PWM system has five synchronized PWMs switching at a non-integer harmonic of the sensor carrier.

#### Introduction

NASA Glenn Research Center (GRC) sponsors flywheel technology development and deployment for spacecraft applications [1]. Flywheel systems can be used for energy storage as an alternative to batteries and reaction wheels in space Also, flywheel modules can be systems. installed in an arrangement which provides both energy storage and momentum control; this kind of system is called an Integrated Power and Attitude Control System (IPACS). A flywheel system is composed of several flywheel modules. along with their supporting electronics. electronics package operates the motor/generators, the MBs and the telemetry.

Energy storage flywheel applications benefit from high energy density, high power density, long life, deep depth of discharge, and broad operating temperature ranges available with flywheels. In an IPACS configuration, an additional mass savings can be achieved through the combination of the energy storage and the attitude control functions into one system.

Flywheel modules for space use are designed to maximize energy density and minimize losses; a representative flywheel module is shown in Figure 1. The flywheel rotor features a high strength carbon fiber rim which stores energy kinetically, and a coaxial motor/generator is used to transfer energy to and from the wheel. The motor, MBs, and touchdown bearings are located on each end of the hub. Stationary components, such as position and temperature sensors, connectors, and wiring harnesses, are located within the housing structure.

The flywheel active MB control system uses a position feedback controller to levitate the rotor by adjusting a set of electromagnets [2]. This controller has five degrees of freedom: two radial degrees of freedom at each end of the rotor and one degree of freedom axially. The radial MB moves the rotor in the X1 and Y1 radial directions, and the combination MB actuates in the X2 and Y2 radial directions, as well as the Z (axial) direction.

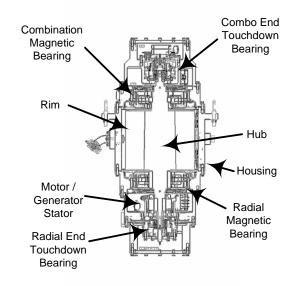


Figure 1. G2 Flywheel Module

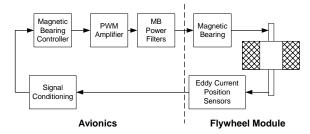


Figure 2. Active MB System

The PWMs drive current through the power filters and into the MB actuators; the resultant magnetic fields in the air gaps between the bearing stator and rotor produce a net force on the rotor, which accelerates, changing its position. Five sets of position sensors measure shaft locations along the MB axes, and this sensor signal is conditioned (scaled, offset and filtered) and passed back to the MB controller, which compares the desired rotor position to the actual position and updates the command signal to the PWMs.

The minimum required closed loop bandwidth of the MB system depends on the flywheel module design; the modules being tested at GRC require control of modes up to 800 Hz. The bandwidth is typically limited by the actuator, power filter and PWM. Other factors which may limit bandwidth are loop time of the digital controller, and sensor signal conditioning. A MB control algorithm which is too complex may not execute in the desired loop time; increasing loop time to allow execution will negatively impact bandwidth. Also, if noise present at the sensors is significant, extensive filtering may be required; lag due to this filtering will also reduce controller bandwidth.

#### **Problem Statement**

Non-contact eddy current position sensors are used to measure rotor location in the flywheel MB control system: these sensors rely on an amplitude modulation (AM) scheme. Switching PWMs are an attractive choice for driving the MB actuators, since they are more compact and less lossy than linear amplifiers; however, incorrect implementation of **PWMs** can contribute significant noise to the position sensor system, making control more difficult. This paper addresses issues that arise with the use of switching PWMs in active MB systems.

Two types of noise which can be generated in the position sensors of a multiple axis PWM MB system are beat frequency noise and demodulation noise. Beat frequency noise is

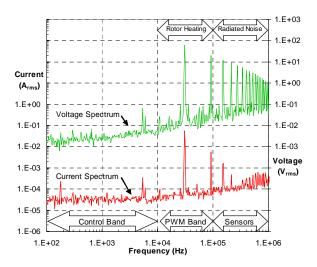


Figure 3. Power Amplifier Spectrum

generated due to variations in individual PWM switching frequencies, and demodulation noise occurs when the PWM switching frequency is selected such that one of its harmonics is near the sensor demodulation frequency.

order to evaluate the impact of this electromagnetic noise on the flywheel system, it is convenient to consider the current and voltage applied by the PWM to the magnetic actuator in the frequency domain (Figure 3). This spectrum can be divided into three general regions: the control band, the PWM band, and the sensor band. The MB control band extends from DC to Ideally, only currents and voltages generated by MB controller commands should be present in this region. The next region up is the PWM switching band, which extends from 10kHz to 100kHz; the fundamental switching frequencies of the PWMs are within this frequency range. The sensor band is the final portion of the spectrum, extending between 100 kHz and 1MHz; the carrier frequency of the eddy current position sensors fall into this range (the sensors used in the GRC flywheels are operated at 500 kHz and 1MHz).

Electromagnetic noise is radiated by operating MB actuators, and measurements have shown that this radiated noise is picked up by the sensors. Although the radiated noise is broad band, we are mainly concerned with noise near the carrier frequency of the sensors. This paper will be limited to measurements on the sensors operating at 500kHz, because they are utilized in the more sensitive control loops. Noise radiated near the 500kHz carrier frequency is detected at the sensor head and demodulated in the eddy current

sensor conditioning electronics, which brings it into the control bandwidth of the MB. For example, a noise peak radiated by a PWM at 499 kHz will appear, after demodulation, as a 1 kHz noise input to the MB controller. Since the control system doesn't significantly attenuate until ~10kHz, we ideally would like a low noise environment in the 490-510 kHz region.

#### **Approach**

The original MB system configuration used separate, non-synchronized PWMs on each of the five control axes, all switching at factory-defined frequencies which varied between 26kHz and 31kHz. This configuration had considerable beating and demodulation noise problems.

Separate techniques were developed to address these two noise types. Beat frequency noise was addressed by synchronizing all of the PWMs on a single oscillator, thus eliminating the variations in switching frequency which cause the noise, and demodulation noise was addressed by choosing the synchronized PWM frequency such that its higher harmonics were distanced from the sensor carrier frequency. A test matrix was developed to test these two methods individually. Relative performance of each method was quantified by recording the MB position sensor noise spectra while levitating the flywheel at 0 RPM, for each of the test cases.

The test matrix details are presented in Table 1. Eight test cases are presented. Test A combines both noise elimination methods, and presents the best case solution, while test H deliberately generates both beat frequency and demodulation Tests B-D are a controlled study the effects of beat frequency noise, and tests E-G study demodulation noise. The tests were designed so that the effects were most evident on the radial (X1-Y1) actuator. In order to simplify data presentation, a single noise spectrum was created for each test case by summing the X1 and Beat frequencies were Y1 spectra together. studied by synchronizing four PWMs at a frequency known not to cause demodulation noise, and moving the frequency of the fifth PWM (X1) in a controlled way. Demodulation noise was generated by synchronizing all five PWMs at various frequencies intended to generate demodulation noise.

Table 1. Noise Testing Matrix

Cell	Test	Config	Harmonic	F <sub>PWM</sub>
Α	best case	synched	15.41n	32,437.6
В	beating	X1	15.41n +50	32,487.6
		Other 4	15.41n	32,437.6
С	beating	X1	15.41n +100	32,537.6
	_	Other 4	15.41n	32,437.6
D	beating	X1	15.41n +200	32,637.6
		Other 4	15.41n	32,437.6
E	demod	All	15n	33,333.3
F	demod	All	15n+45	33,336.3
G	demod	All	15n+90	33,339.3
Н	beating &	X1	15n+90+50	33,389.3
	demod	Other 4	15n+90	33,339.3

#### Results

All cases in the test matrix described in Table 1 were run. In this section, details of each test are given, and results are presented. Performance of best and worst case configurations is discussed, and comments on system configuration beyond the PWM noise setup (i.e. grounding and shielding) are provided.

#### Beat Frequency Noise

When PWM amplifiers with different switching frequencies are used to drive coils in the same MB actuator, beat frequency noise can result; this noise is picked up by the position sensors for that plane.

Test cells B, C, and D illustrate the beat frequency noise effect; this test is summarized in Table 2. For these tests, the PWMs for the Y1, X2, Y2, and Z axes are all synchronized at 32.437 kHz; this frequency was specifically selected to minimize the other major noise source (demodulation noise). The X1 PWM switching frequency was then varied from the nominal frequency by 50, 100, and 200 Hz.

Results of test cells B-D are plotted in Figure 4. Distinct beat frequencies can easily be observed, one for each test case, at 50, 100 and 200 Hz. Note that the magnitude of the beating is greatest when the PWM frequencies are closest (test B).

Table 2. Beat Frequency Test Matrix

Tomate at a contribution of the contribution o				
Cell	Test	Config	Harmonic	F <sub>PWM</sub>
В	beating	X1	15.41n +50	32,487.6
		Other 4	15.41n	32,437.6
С	beating	X1	15.41n +100	32,537.6
		Other 4	15.41n	32,437.6
D	beating	X1	15.41n +200	32,637.6
		Other 4	15.41n	32,437.6

Noise from the utility power is also present on all of the sensor spectra. It can be seen at its fundamental of 60Hz, and at its harmonics; in Figure 4 the fundamental, second, and third harmonics can be easily seen.

#### **Demodulation Noise**

The PWMs used in these tests were the two-state type, operated on an 80V DC bus. When a zero current is commanded on this type PWM, it generates a square wave of 50% duty cycle. This voltage is applied to the MB actuators, and the resulting currents have content at the switching frequency and its harmonics. A Fourier decomposition of this square waveform was done to determine the theoretical magnitude of the voltage at frequencies near the demodulation frequency of the position sensors. The ideal square wave and the function reconstructed from summing the first nineteen terms of the Fourier series are shown in Figure 5 (note that square waves contain only odd harmonics). There is still content in the 15<sup>th</sup> harmonic; this is the region of interest, as radiated noise from a single (or multiple) PWM at these frequencies can be demodulated into the control band by the sensor system, and introduced to the MB control algorithm.

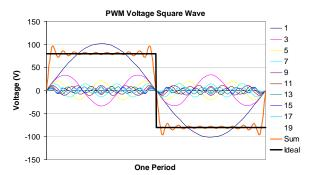


Figure 5. 80V Square Wave (Theoretical)

Figure 6 shows the output voltage frequency spectrum of a two stage PWM, fundamental switching frequency 30,600 Hz, run on an 80 VDC source (solid line), along with the theoretical 80 VDC harmonic voltage magnitudes (diamonds). The frequency of each harmonic is shown above each peak, and the harmonic number is shown below. Note that the actual spectrum follows the theoretical, although it gradually drops away from the ideal calculation due to line inductance and second order effects.

The carrier frequency of the position sensors of interest in the GRC system is 500kHz. The 15<sup>th</sup> and 17<sup>th</sup> harmonics bracket the carrier frequency in the example system plotted in Figure 6.

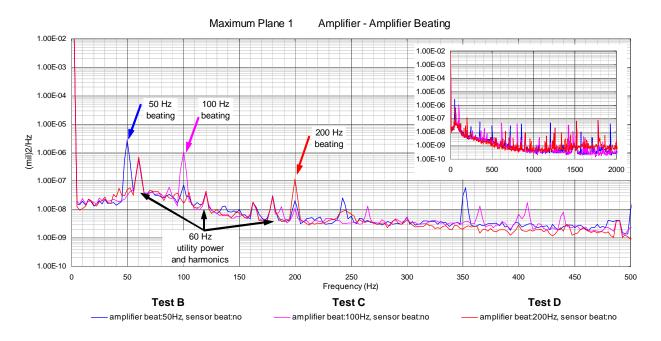


Figure 4. Beat Frequency Noise Spectrum

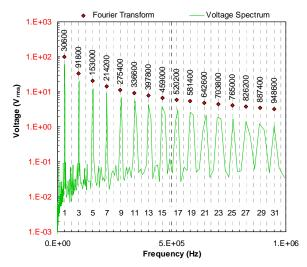


Figure 6. Actual vs. Theoretical PWM Voltage (80 V bus)

A worst case scenario for demodulation noise would be selection of the PWM switching frequency such that one of its harmonics was an odd integer multiple of the sensor carrier frequency, or

$$F_{sensor}/F_{pwm} = n$$
 (1)

where n is an odd integer. A series of test cases were run to quantify this effect; the test is summarized in Table 3. All five PWMs were synchronized for these tests; the switching frequency was set so the 15<sup>th</sup> harmonic was

exactly 500kHz, per Equation 1, in test E. The switching frequency was then bumped up by 3 and 6 Hz in tests F and G, which correspond to 45 Hz (3Hz\*15<sup>th</sup> harmonic) and 90Hz changes at the demodulation frequency. Cell A is the best case scenario for this test, with all of the PWMs synchronized to a non-integer harmonic below the 15<sup>th</sup>.

Table 3. Demodulation Frequency Noise Test

Cell	Test	Config	Harmonic	F <sub>PWM</sub>
Α	best case	synched	15.41n	32,437.6
E	demod	All	15n	33,333.3
F	demod	All	15n+45	33,336.3
G	demod	All	15n+90	33,339.3

Figure 7 shows the results for the demodulation noise and best case tests. The best case (cell A) spectrum has peaks only at the utility power frequency (60Hz) and its harmonics. Due to low frequency measurement limitations of the spectrum analyzer, it is difficult to see all of the effects in the spectral measurement for cell E; however, a broad shoulder can be seen between 10-50 Hz for this test cell. Cell F is an excellent illustration of the demodulation noise effect with a strong demodulation frequency at 45Hz, and test G shows demodulation noise at 90Hz and its harmonics; the second through fifth harmonics can easily be seen in the Test G data.

Ideal selection of the synchronized PWM switching frequency would place the sensor demodulation frequency well within the two

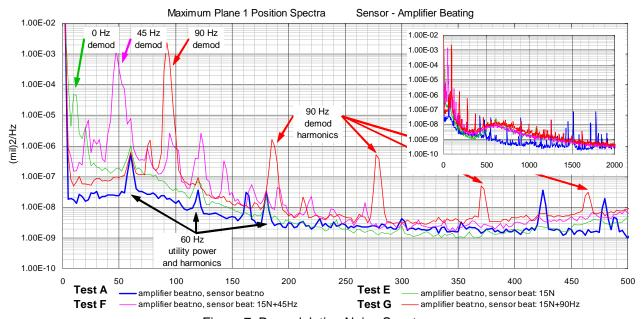


Figure 7. Demodulation Noise Spectrum

nearby PWM harmonics. Figure 8 was generated to allow easy visualization of this selection process. The sensor carrier frequency is plotted along the vertical axis, and the possible PWM frequencies, along the horizontal. Each individual black line plotted on the chart represents an odd harmonic of the PWM frequency plotted as a sensor frequency vs. the PWM fundamental. Thus the lowest line on the chart has slope 1, then next, slope 3, etc. Since our sensor carrier frequency is 500kHz, the ideal PWM switching frequency would be selected by drawing a line up from the horizontal axis, and choosing a point on the 500kHz sensor carrier line which is halfway between two harmonic lines.

Our commercial PWMs are limited to switching frequencies between 31 - 34 kHz, which places us between the  $15^{th}$  and  $17^{th}$  harmonics, per Figure 8. During testing, the harmonic number selected was n = 15.41, or  $F_{PWM} = 32,437.6$  Hz, because this frequency does not have any odd integer PWM harmonics near the carrier frequency. This test frequency is plotted on Figure 8 in blue. It was selected empirically, before Figure 8 was developed; note that a PWM frequency closer to 31kHz would be a better selection, as it would be closer to the center point between the 15ht and  $17^{th}$  harmonics.

### Best vs. Worst Configuration

The final comparison that was made was between the best and worst case configurations, as described in Table 4. In the best case for this testing, all five PWMs were synchronized, and the switching frequency was not an odd integer multiple of the position sensor demodulation; this is the selected configuration for the GRC flywheel modules. In the worst case for this test, the X1 PWM was set 50 Hz above the other four PWMs to induce beat frequency noise, and the remaining PWMS were set such that the 15<sup>th</sup> harmonic was 90 Hz above the sensor carrier frequency. Note that this is by no means the worst-case configuration possible - if the other four PWMs were not synchronized, multiple sources of both types of noise could be generated; however, noise sources would be difficult to separate under these conditions. Thus, cell H represents the worst case for a controlled test.

Table 4. Best and Worst Configuration Test

Cell	Test	Config	Harmonic	F <sub>PWM</sub>
Α	best case	synched	15.41n	32,437.6
Н	beating & demod	X1 Other 4	15n+90+50 15n+90	33,389.3 33,339.3

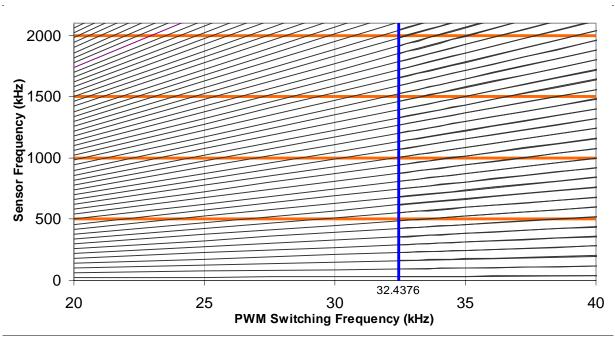


Figure 8. Synchronized PWM Switching Frequency Selection

Figure 9 shows the best vs. worst case results. In the best case, the 60Hz line noise and its harmonics is the most discernable noise source. The worst case configuration shows both the beat frequency and demodulation noise effects; note that many other noise frequencies also arise from interactions between these effects. In the inset graph the higher noise floor can be seen across the frequency range, particularly in the range between 300 and 1500 Hz.

#### Impact of Grounding and Shielding

The data for this paper was collected two times, once when the initial observations were made and a second time for presentation quality data. During the interval between those tests the quality of the grounding and shielding setup for the flywheel module and its power electronics system was improved dramatically. A single point ground was employed, and a much larger fraction of the power and signal cables were converted to twisted shielded pairs. These changes reduced the magnitude of the effects observed in this paper significantly from the first work to the final data set, but allow for a lower noise environment overall.

#### Conclusions

Switching PWMs produce interference with eddy current position sensors. Two separate noise types were characterized – beat frequency noise and demodulation noise.

Beat frequency noise arises when multiple PWMs with different switching frequencies operate on a common MB actuator. This effect can be eliminated by synchronizing all of the PWMs in the system.

Demodulation noise is generated when odd harmonics of the PWM switching frequency fall near the carrier frequency of the position sensors. This problem can be avoided by selecting the PWM frequency such that no odd harmonics fall on the sensor demodulation frequency.

The selected configuration for the GRC flywheel modules, based on the study performed in this paper, has all five PWMs synchronized, and switching at a non-integer harmonic of the position sensor carrier frequency.

#### References

[1] McLallin, K., Jansen, R., Fausz, J., Bauer, R., "Aerospace Flywheel Technology Development for IPACS Applications," NASA TM-2001-211093, October 2001.

[2] Dever, T. P., Palazzolo, A. B., Thomas, E. M., and Jansen, R. H., "Evaluation and Improvement of Eddy Current Position Sensors in Magnetically Suspended Flywheel Systems," *July 2001 IECEC Conference Proceedings*, Savannah, Georgia, 2001.

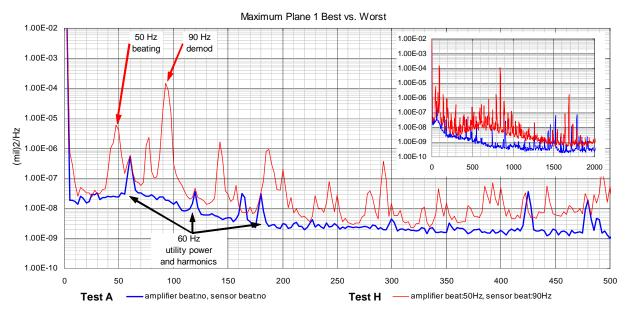


Figure 9. Demodulation and Beat Frequency Noise vs. Best Case

### REPORT DOCUMENTATION PAGE

Form Approved OMB No. 0704-0188

Public reporting burden for this collection of information is estimated to average 1 hour per response, including the time for reviewing instructions, searching existing data sources, gathering and maintaining the data needed, and completing and reviewing the collection of information. Send comments regarding this burden estimate or any other aspect of this collection of information, including suggestions for reducing this burden, to Washington Headquarters Services, Directorate for Information Operations and Reports, 1215 Jefferson Davis Highway, Suite 1204, Arlington, VA 22202-4302, and to the Office of Management and Budget, Paperwork Reduction Project (0704-0188), Washington, DC 20503.

1. AGENCY USE ONLY (Leave blank) 2. REPORT DATE 3. REPORT TYPE AND DATES COVERED			res covered
	December 2003	Technic	cal Memorandum
i. TITLE AND SUBTITLE 5. FUN			JNDING NUMBERS
PWM Switching Frequency Suspended Flywheel System	Effects on Eddy Current Senso s		
6. AUTHOR(S)			WBS-22-755-60-12
Ralph Jansen, Ramon Lebro	n, Tim Dever, and Art Birchenc	ough	
7. PERFORMING ORGANIZATION NA	ERFORMING ORGANIZATION		
National Aeronautics and Sp John H. Glenn Research Cen Cleveland, Ohio 44135–319	E-14180		
9. SPONSORING/MONITORING AGEN	CY NAME(S) AND ADDRESS(ES)		SPONSORING/MONITORING
National Aeronautics and Sp Washington, DC 20546–000	NASA TM — 2003-212622 AIAA–2003–6107		
11. SUPPLEMENTARY NOTES			
Aeronautics and Astronautic Ohio 43606; Ramon Lebron	ntional Energy Conversion Engi s, Portsmouth, Virginia, August and Art Birchenough, NASA C ponsible person, Ralph H. Janso	t 17–21, 2003. Ralph Jansen, Glenn Research Center; and T	im Dever, QSS Group, Inc.,
12a. DISTRIBUTION/AVAILABILITY S	<b>FATEMENT</b>	12b.	DISTRIBUTION CODE
Unclassified - Unlimited Subject Categories: 20, 33, 3	7, and 44 Distrib	oution: Nonstandard	
Available electronically at http://g	gltrs.grc.nasa.gov		
	the NASA Center for AeroSpace Int	formation, 301–621–0390.	
noise generated by the PWM noise caused by variations in harmonics of the switching v PWM switch frequencies, an have harmonics at the carrier	g (MB) pulse width modulated is in the flywheel position sense. PWM switching frequencies, a roltage into the MB control band demodulation noise is minim	or system. Two types of noise and demodulation noise caus and. Beat frequency noise is eluized by selection of a switch	
14. SUBJECT TERMS			15. NUMBER OF PAGES
Flywheels; Reaction wheels; Counter-rotating wheels; Electric motors;			13
Electromechanical devices			16. PRICE CODE
17. SECURITY CLASSIFICATION OF REPORT Unclassified	8. SECURITY CLASSIFICATION OF THIS PAGE Unclassified	19. SECURITY CLASSIFICATION OF ABSTRACT Unclassified	20. LIMITATION OF ABSTRACT
Uliciassilieu	Uliciassificu	Unclassined	1